EVAPORATION FROM DROPS CONTAINING DISSOLVED SOLIDS

D. H. CHARLESWORTH and W. R. MARSHALL, JR., University of Wisconsin, Madison, Wisconsin

A study was made of the evaporation from single drops containing solids. By means of a specially designed sensitive balance, drops were suspended over a hot-air stream and their drying behavior was observed. Weight changes were measured during evaporation. Experimental data are presented on the time of appearance of the first solid phase and the formation of a solid crust for a wide range of drying conditions and materials. A theory is advanced for predicting the formation of a solid phase in drying a droplet containing a dissolved solid. This theory shows reasonable agreement with the experimental results. A tentative proposal for the application of the results to spray-dryer performance is suggested.

PART I

The aim of the investigation reported here was to develop a method of predicting the drying rates of drops containing dissolved solids for application to design calculations for spray dryers and to obtain fundamental information on the phenomena occurring during the drying process. Considerable attention was given to the problem of predicting the formation of a solid phase in drying a droplet of an inorganic salt solution. The need for such information has become more pressing as spray-drying techniques have become widely applied to the production of dried foodstuffs, pharmaceuticals, and tonnage chemicals.

As in most drying operations, the spray-drying process can be subdivided into periods. The first period is characterized by evaporation from a free liquid surface, the second by evaporation from or through a solid structure which forms at an intermediate point in the process. Accordingly this study was divided into the following sections: (1) evaporation rates and droplet conditions during the first period of drying, (2) formation of the solid phase about the droplet, and, (3) evaporation rates during the second period of drying.

REVIEW OF PREVIOUS WORK

Studies of the evaporation of pure-liquid droplets can be related directly to the first period of spray drying. The theory of evaporation into still air has been treated by Fuchs (*6*) and Luchak and Langstroth (*9*). Experimental verification of the relationships for a number of pure liquids was carried out by Ranz and Marshall (*10*) and by Langstroth *et al.* (*8*). Studies of the evaporation of pure-liquid drops having a finite velocity relative to the surrounding air were made by Frössling (*5*) and by Ranz and Marshall (*10*).

Information on the evaporation from droplets containing solids and on the formation of a solid phase is sparse. Ranz and Marshall (*10*) in addition to their work with pure liquids presented some observations of evaporation from droplets of solutions and suspensions and concluded that if the presence of the solid affects the vapor pressure, drying proceeds during the first period as if the entire droplet were saturated. The investigation also included measurements of the temperature history of droplets containing suspended or dissolved solids evaporating in still air.

The mechanism of the drying of small particles such as are encountered in spray drying has received little attention with the exception of the manner in which hollow particles are formed, a number of investigators (*2, 4, 7, 10*) having hypothesized reasons for the occurrence of internal voids.

THEORETICAL CONSIDERATIONS

The complexity of the process of evaporation from a droplet having a velocity relative to the surrounding air is greatly increased by the presence of nonvolatile dissolved solids in the droplet. Whereas, in the consideration of heat and mass transfer from a droplet of pure liquid, conditions within the droplet may justifiably be assumed uniform, they cannot be if there is a nonvolatile material present.

In general the concentration of solute is initially uniform in the droplet; however as soon as some evaporation has taken place from the droplet surface, concentration gradients are set up and there is diffusion of solvent toward the surface and solute toward the center. In addition, since the drop is necessarily decreasing in size, the solute in the surface layer is swept inward by the retreating interface, which is impermeable to the solute.

If the evaporation rate were constant over the entire surface, as would be the case for zero relative velocity between the droplet and the surroundings, the concentration gradients within the droplet should have spherical symmetry. However if the relative velocity is not zero, boundary-layer theory predicts, and Frössling (*5*) has demonstrated experimentally, that the evaporation rate varies from a maximum at the point of impingement at the front of the drop, through a minimum at some latitude beyond the equator, to a second but lower maximum at the rear. As a result, diffusion has a tangential component toward the rear of the drops in addition to the radial one. The concentration profiles are consequently not simple.

Superimposed on the flow, owing to diffusion, may be internal circulation from density gradients caused by temperature and concentration and from the viscous drag of the passing air. Droplet rotation as a whole may also be present. The latter, if sufficiently rapid and random, would tend to restore the spherical symmetry. If, however, the droplet initially has no rotational motion and its relative velocity is in the direction of gravity, the maximum evaporation rate at the front of the droplet results in a high concentration of solute in that area. This ordinarily implies a greater than average density at the front of the drop, a situation which could add to the stability against rotation.

It is postulated that the surface solute concentration does not remain uniform but rather rises smoothly from its initial value. Since the rate of evaporation is almost constant (depending on the vapor pressure-concentration relation and any changes in the Reynolds number of the flow) and the surface concentration is increasing, the rate of accumulation at the surface increases. When the surface concentration reaches the saturation value, it can no longer continue to increase and solute must be deposited as a solid phase. Consequently, if the surface concentration of solute could be expressed as a function of time and drying conditions, the time of formation of the solid phase could be predicted. If rigorous, such a function would be complicated by the lack of spherical symmetry and by internal circulation.

Using this concept of the process as a basis and assuming internal transfer by diffusion only, one can express the

D. H. Charlesworth is with Atomic Energy of Canada, Limited, Chalk River, Ontario, Canada.

surface concentration of solute as a function of time and drying conditions and estimate the time of formation of the solid phase. Such a function should also take into account the lack of spherical symmetry in and around the droplet, as well as internal circulation. Their inclusion, however, renders the problem so complex as to be insoluble. The solution of the simplified problem cannot be expected to predict values accurately, but the form of the solution should be useful in the correlation of experimental data.

A formulation of the problem is best accomplished by considering a synthetic model which most closely approximates the drying droplet and yet is sufficiently simple to be expressed in a usable mathematical form. If transfer in the droplet by diffusion only is assumed, together with spherical symmetry, then the radial diffusion equation in spherical coordinates may be used as the basic differential equation. One of the boundary conditions results from the practical situation that the droplet is initially of uniform concentration. The second boundary condition must express the accumulation of solute in the surface layer of the droplet resulting from water evaporation and droplet shrinkage. Since a moving boundary presents serious mathematical difficulties, the model droplet is considered to be of constant diameter and to be receiving solute through the surface in an amount per unit time equal to the solute in a surface layer of volume equivalent to the actual drop volume decrease per unit time.

Mathematically this boundary-value problem becomes

$$\frac{\partial c}{\partial \theta} = D\left(\frac{\partial^2 c}{\partial r^2} + \frac{2}{r}\frac{\partial c}{\partial r}\right) \quad (1)$$

The boundary conditions may be written

$$c(r,\theta) = c_o \quad 0 < r < x_o/2 \quad (2)$$

$$D\left(\frac{\partial c}{\partial r}\right)_{r=x/2} = \frac{-\frac{dm}{d\theta}\cdot\bar{v}\,c}{\pi x^2} \quad (3)$$

A practical approximation in most cases is that the evaporation rate $dm/d\theta$ from a droplet of solution is equal to that from a pure-water droplet of the same size.

For an evaporating droplet of pure liquid

$$-\frac{d(x^2)}{d\theta} = -\frac{dm}{d\theta}\cdot\frac{4\bar{v}}{\pi x} \quad (4)$$

At low Reynolds numbers and for small ranges of x, $[d(x^2)]/d\theta$ may be considered constant. An evaporation constant K is therefore defined by

$$-\frac{d(x^2)}{d\theta} = 8K \quad (5)$$

or

$$-\frac{dm}{d\theta} = \frac{2\pi x K}{\bar{v}} \quad (6)$$

Substituting Equation (6) into Equation (3) yields

$$\left(\frac{\partial c}{\partial r}\right)_{r=x/2} = \frac{2\beta c}{x} \quad (7)$$

Solution of Equations (1), (2), and (7) leads to

$$c(r,\theta) = 2c_o\beta\left[\frac{\cosh\phi\,\sinh\left(\frac{2\phi r}{x}\right)\exp\left(\frac{-4\phi^2 D\theta}{x^2}\right)}{\phi\,(\sinh^2\phi - \beta)} - \sum_{n=1}^{\infty}\frac{\cos\alpha_n\,\sin\left(\frac{2\alpha_n r}{x}\right)\exp\left(\frac{-4\alpha_n^2 D\theta}{x^2}\right)}{\alpha_n(\sin^2\alpha_n + \beta)}\right] \quad (8)$$

where

ϕ is the positive real root of

$$\tanh y = \frac{y}{\beta+1} \quad (8a)$$

and

α_n $(n = 1, 2, 3, \ldots)$ are the positive real roots of $\tan z = \frac{z}{\beta+1}$ (8b)

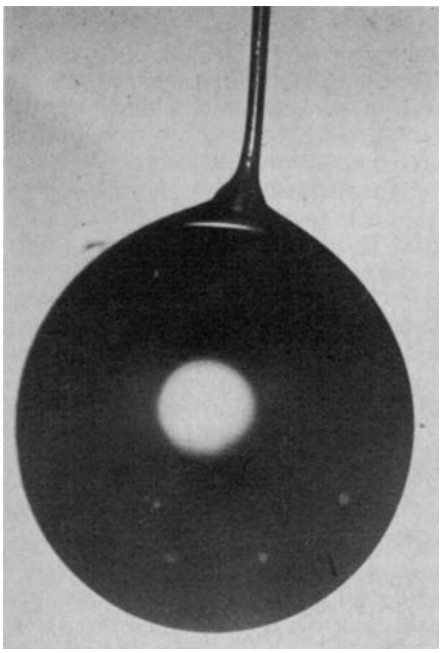

Fig. 1. Suspended drop.

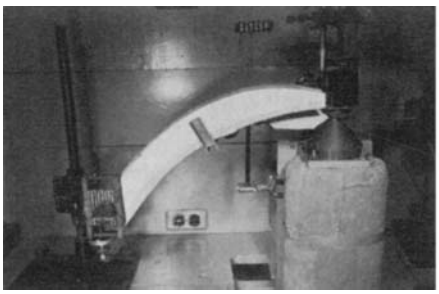

Fig. 2. Drop balance.

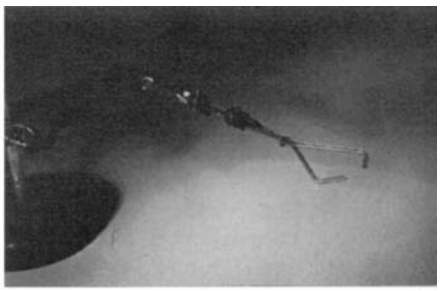

Fig. 3. Drop-suspension and thermoelement combination.

Compensation for changing drop size is made by inserting the relation

$$x^2 = x_o^2 - 8K\theta \quad (9)$$

Since it is postulated that a solid phase appears as soon as the surface becomes saturated, the time of the formation of a solid phase about the droplet will be that at which

$$c(x/2,\theta_c) = c_s \quad (10)$$

Equation (10) is much too complicated to be satisfactorily solved for θ_c. Fortunately several compensatory approximations can be made to render a solution possible. Calculation omitting the terms under the summation sign yields a somewhat high value of $c(x/2,\theta)$. This discrepancy is counteracted to a large extent by replacement of $(2\beta\cosh\phi\,\sinh\phi)/[\phi(\sinh^2\phi - \beta)]$ by unity. The simplified expression is then

$$c(x/2,\theta) = c_o\exp\left[\frac{4\phi^2 D\,\theta}{x_o^2 - 8K\theta}\right] \quad (11)$$

It can be seen that the two approximations are exactly compensating

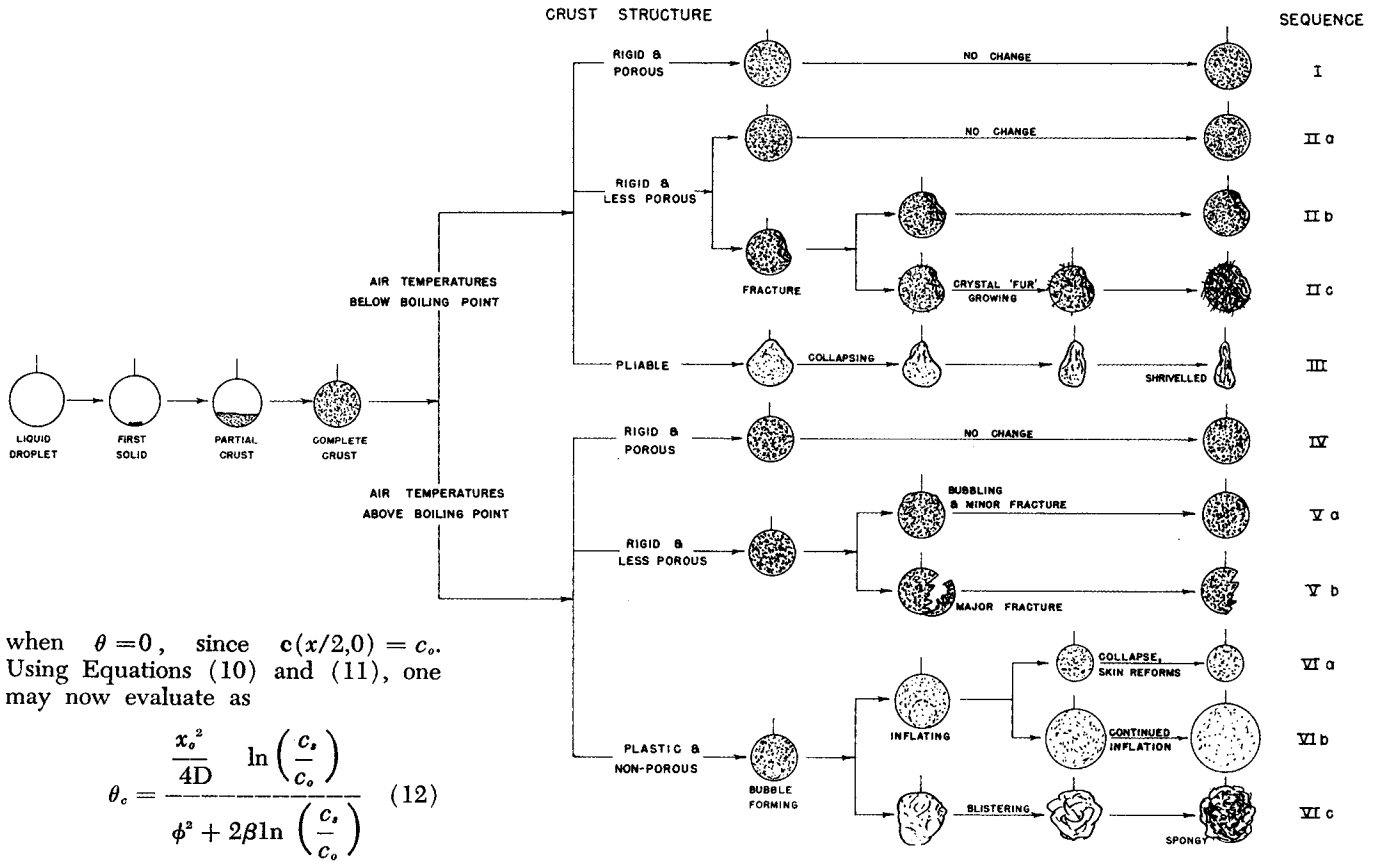

Fig. 4. Appearance changes in drying droplets.

when $\theta = 0$, since $c(x/2,0) = c_o$. Using Equations (10) and (11), one may now evaluate as

$$\theta_c = \frac{\dfrac{x_o^2}{4D} \ln\left(\dfrac{c_s}{c_o}\right)}{\phi^2 + 2\beta \ln\left(\dfrac{c_s}{c_o}\right)} \qquad (12)$$

A convenient substitution for calculation is $c_s/c_o = (\rho_s C_s)/(\rho_o C_o)$.

Equation (12) will be used as a correlating equation for experimental data concerning the formation of a solid phase about a droplet.

EXPERIMENTAL EQUIPMENT AND PROCEDURES

For study of the drying of droplets of aqueous solutions, a technique was developed wherein an individual droplet was suspended in a controlled air stream, and its weight or temperature was measured as the drying progressed. Visual observations of the appearance and size of the particle were recorded.

Control and Measurement of Air Stream Conditions

The metering and control of the test air stream were accomplished with essentially the same equipment used by Ranz and Marshall (*10*) with the exception that the 140-mesh screen on the convergent nozzle over which the drop was suspended was omitted, since it was easily clogged by stray droplets of solution.

Droplet Formation and Suspension

The droplets to be dried were formed from a microburette, the tip of which was fitted with a glass capillary tube of approximately 275-μ diameter thoroughly coated inside and out with Dri-film to facilitate the transfer of the droplet to the suspension filament. The transfer was accomplished by picking the droplet from the tip of the burette with a horizontally held glass filament, touching it to the end of the suspension filament, then drawing the transferring filament out through it. This allowed the droplet to slide off one filament and be left clinging to the other.

The suspension adopted was a vertical glass filament, the tip of which was drawn to small diameter and then touched to a flame to give a small knob on the end. Typical diameters were 340μ for the main filament, 70μ for the necked-in portion, and 200μ for the knob. The upper portion of the knob and the adjoining filament were coated with Dri-film to prevent the droplets from climbing the filament, but sufficient wettable area was left to support the droplet. The vertical positioning of the filament with the air stream blowing up from below minimized flow disturbances and eliminated transverse convection currents in the jet.

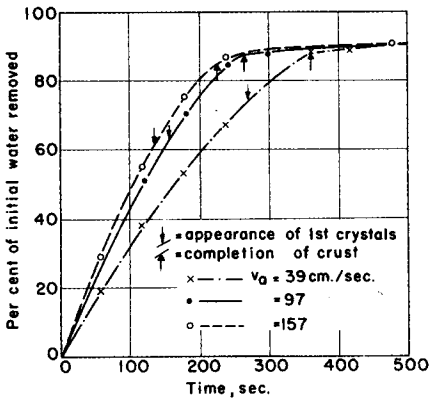

Fig. 5. Effect of air velocity on drying aqueous sodium-sulfate drops $t_a = 94°F.$, $x_o = 0.1565$ cm., $C_o = 0.082$ g./g. solution.

The surface of a drop suspended from the filament intersected the knob approximately at its equator as shown in Figure 1. The immersed portion of the knob, therefore, added only about 0.1% to the volume of a 2- by 10^{-3}-ml. droplet, the size most frequently used in the investigation. The cross-sectional area of the knob amounted to just 0.5% of the droplet area. It was estimated that the heat conducted to the droplet along the filament did not exceed 1% of the total heat input to the droplet.

Measurement of Droplet Weight

The visual technique of measuring evaporation rates from pure-liquid drops (*10*) is not admissible to the study of drops around which a solid structure has formed. For this study the balance shown in Figure 2 was developed, whereby the weight of a suspended droplet could be measured at intervals throughout the course of the drying. The main element of the balance was a glass filament 43 cm. in length tapered from a diameter of 425μ at its fixed end to 210μ at its free end. The large end was fixed to the vertically travelling micrometer stage of a cathetometer. Welded at right angles to the free end was a 3.2-cm. suspension filament of the type described above. As mounted, the

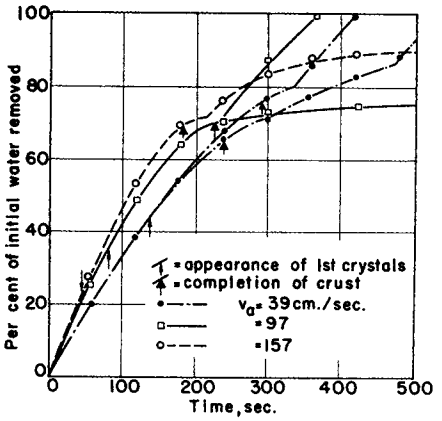

Fig. 6. Effect of air velocity on drying aqueous sodium-sulfate drops $t_a = 94°F.$, $x_o = 0.1565$ cm., $C_o = 0.164$ g./g. solution.

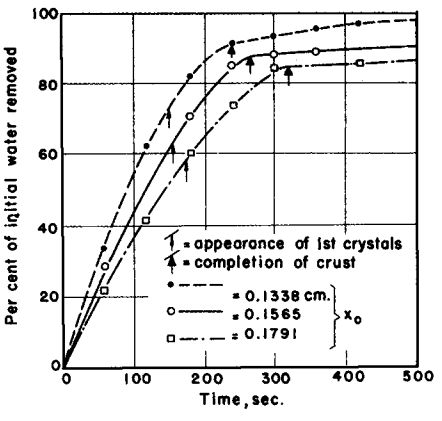

Fig. 7. Drying of aqueous sodium sulfate drops of different initial diameters $t_a = 94°F.$, $v_o =$ 97 cm./sec., $C_o = 0.082$ g./g. solution.

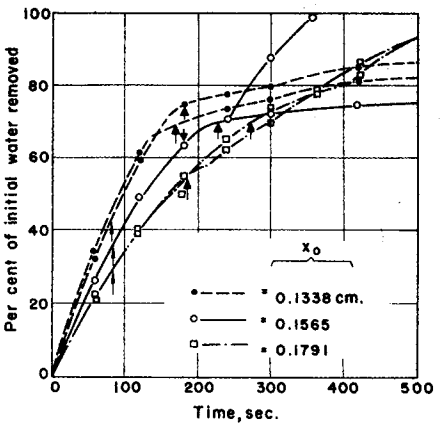

Fig. 8. Drying of aqueous sodium sulfate drops of different initial diameters $t_a = 94°F.$, $v_a =$ 97 cm./sec., $C_o = 0.165$ g./g. solution.

fixed end of the weighing filament was inclined at 45 deg., whereas the free end came to rest under its own weight in an almost horizontal position. Under the weight of a droplet suspended on it the free end of the filament deflected a distance which was a unique function of the drop weight. The amount of deflection could be determined by measuring the vertical distance through which it was necessary to raise the fixed end of the filament so that the free end was restored to its zero position. The drop weight could then be determined from a calibration curve relating weight to deflection. The calibration curve was almost linear and showed that the filament deflected an average of 12.8 mm./mg. and had a capacity of 4.0 mg., approximately the weight of a 1,970-μ drop. It was estimated that changes in drop weight could be measured within ± 0.01 mg.

To permit weighing of a droplet evaporating in flowing air from the nozzle, a deflecting shield was swung over the nozzle opening at the time a weight reading was made.

Measurement of Droplet Temperature

Figure 3 shows the suspension and thermoelement combination used for runs in which the temperature history of the droplet was recorded. It consisted of a fork of glass tubing, to hold the thermocouple, and a suspension filament. The thermoelement was formed from ½-ml. manganin and constantan wires and was connected to a quick-response recording potentiometer.

Visual Observation System

During all runs the evaporating droplets were observed under magnification from two perpendicular directions, in silhouette on the ground glass of a microscope camera and by reflected light in a microscope fitted with a micrometer eyepiece.

Experimental Procedures

It was impractical to measure the droplet temperature and its weight loss during the same experiment. Parallel runs under identical conditions therefore measured mass transfer in one and drop temperature in the other.

Mass transfer data in the form of a weight history of a droplet were obtained. Under most conditions the particle was weighed at 1-min. intervals. The time during which the air flow was cut off from the particle to permit one weighing was about 10 sec. and was not included in the recorded drying time. A change in the number or spacing of weighings did not noticeably affect the results.

The recorded temperature histories of the droplets were continuous, since there was no necessity for interrupting the air flow to obtain readings.

The drying particle was kept under almost continuous observation during that portion of the drying in which significant changes in appearance could be detected. Special notice was made of the times at which the solid phase first appeared and at which it completely encased the particle.

Materials and Range of Conditions Studied

Weight loss, temperature history, and time necessary for solid formation were measured for droplets of a number of aqueous solutions and suspensions. Parallel sets of runs under similar conditions in which weight loss and temperature history were measured were made with aqueous solutions of the following materials with initial solute concentrations as indicated; sodium sulfate (8.2 and 16.4 wt. %), potassium sulfate (5.3 and 10.7 wt. %), copper sulfate (10.7 wt. %), ammonium nitrate (12.5, 25.0 and 50.0 wt. %), calcium chloride (10.0, 19.4, 30.0, and 41.0 wt. %), sodium acetate (12.4 and 25.0 wt. %), and coffee extract (26.0 wt. % solids).

A variety of aqueous solutions and suspensions were dried as individual droplets under close observation with regard to solid-phase formation and general appearance during drying. No droplet weights or temperatures were recorded, only drying conditions. Included in this group were ammonium sulfate, ammonium chloride,

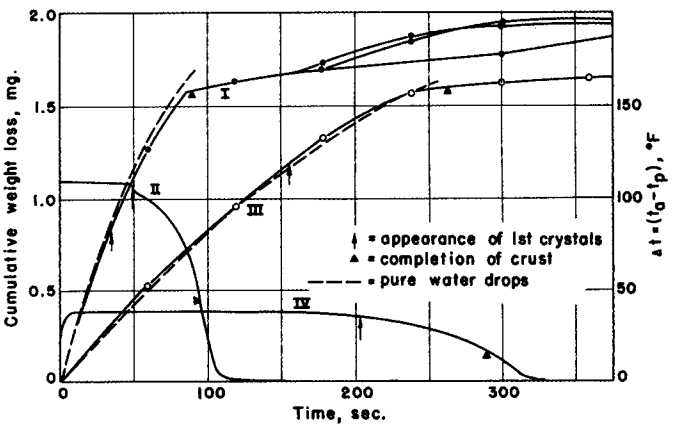

Fig. 9. Effect of temperature on the drying of drops of sodium sulfate solution; $x_o = 0.1565$ cm., $C_o = 0.082$ g./gm. solution.
I. Cumulative weight loss, $t_a = 197°F.$, $v_a = 117$ cm./sec.
II. Temperature difference, $t_a = 191°F.$, $v_a = 114$ cm./sec.
III. Cumulative weight loss, $t_a = 94°F.$, $v_a = 97$ cm./sec.
IV. Temperature difference, $t_a = 93°F.$, $v_a = 97$ cm./sec.

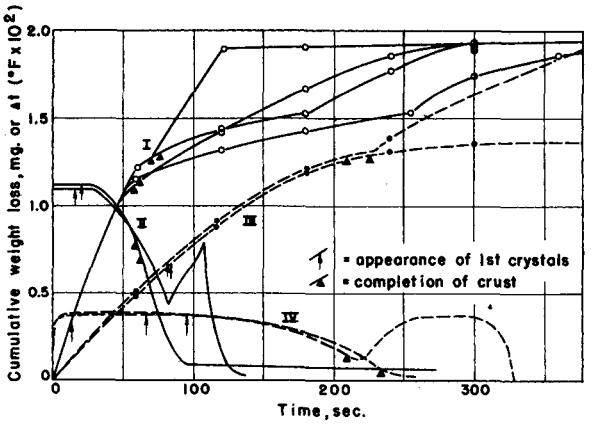

Fig. 10. Effect of temperature on the drying of drops of sodium sulfate solution; x_o = 0.1565 cm., C_o = 0.164 g./g. solution.

I. Cumulative weight loss, t_a = 197°F., v_a = 117 cm./sec.
II. Temperature difference, t_a = 193°F., v_a = 114 cm./sec.
III. Cumulative weight loss, t_a = 94°F., v_a = 97 cm./sec.
IV. Temperature difference, t_a = 94°F., v_a = 97 cm./sec.

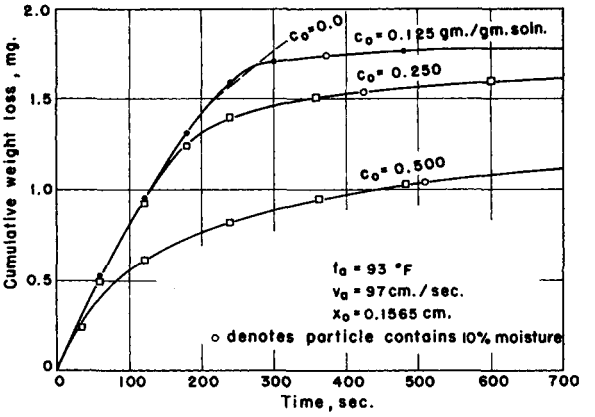

Fig. 11. Effect of initial concentration on the drying of drops of ammonium nitrate solution.

sodium chloride, potassium nitrate, lithium hypochlorite, sucrose, a dispersible blue dye, whole fresh milk, and a dispersion of polyvinyl acetate resin in water.

The experimental techniques required the use of drying conditions which produced relatively slow rates of evaporation. The majority of the work was done at moderate air temperatures and velocities and with large droplets. Unfortunately, these are not the conditions usually encountered in practical spray drying. Where possible, practical conditions were approached. Tests were carried out over as wide a range of the variables as the techniques and apparatus would permit in order to aid the extrapolation of the experimental data to commercial conditions.

The ranges of variables under which droplets were dried were

Air temperature	88° to 318°F
Air velocity	39 to 157 cm./sec. (1.2 to 5.2 ft./sec.)
Droplet volume	125 x 10^{-5} to 300 x 10^{-5} ml.
Droplet diameter	1.3 to 1.8 mm.
Initial solute concentration	5.3 to 50 wt. %
Ratio of initial concentrate to saturation concentration	0.18 to 0.89

EXPERIMENTAL RESULTS AND THEIR CORRELATION

General Appearance of Droplet During Drying

A generalized description of the appearance of a suspended droplet of an aqueous solution of an inorganic salt drying under conditions similar to those used in this investigation will be useful in understanding the experimental data obtained (Figure 4). Up to a point the sequences of events which were observed were similar for all droplets no matter what the solute or the drying conditions. During the first portion of the drying the droplet decreased in size with no appearance of a solid phase. The presence of a solid phase was first evidenced by the formation of crystals at the bottom of the drop. As drying progressed, more crystals appeared, forming a surface crust which grew steadily up the sides of the droplet. If the droplet did not rotate, the advancing front of the crust remained symmetrical about the vertical axis and continued to rise until the droplet was completely encased in a layer of solid material. The rate of advance of the solid front was initially relatively fast. It slowed markedly as it approached the droplet equator; then, once past it, it speeded up, completing the upper half of the crust in appreciably less time than was required for the formation of the lower portion. If the drop (or its surface) rotated, swinging the solid up the side of the drop, there was a strong tendency for the crust to re-form in its previous position. That portion of the crust which bodily advanced past the latitude of the old solid front rapidly redissolved. Also the crust quickly grew over any liquid surface which was exposed below the normal front latitude. The redissolution process was in general more rapid than the reformation process.

The results of further drying after the completion of the crust about the droplet differed depending on the nature of the solute and the surrounding air temperature.

If the air temperature was below

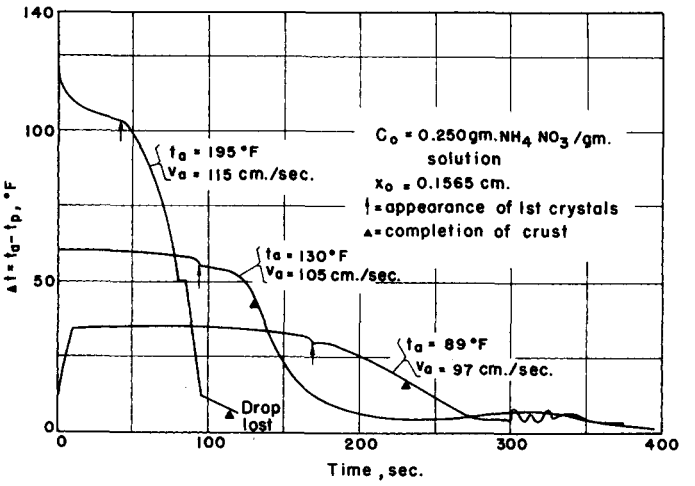

Fig. 12. Effect of temperature on the drying of drops of ammonium nitrate solution.

the boiling point of the solution, several different phenomena were possible. If the crust was rigid and quite porous (sequence I, Figure 4), its appearance did not change appreciably with further drying. The liquid-vapor interfaces retreated into the pores between the crystals. This retreat could be detected by a twinkling within the crust. Examples of such behavior were observed in the drying of potassium sulfate, ammonium chloride, and sodium chloride solutions. If the crust was rigid but not too porous (sequence II), stresses set up by the further crystal growth or by the surface tension of the liquid phase often

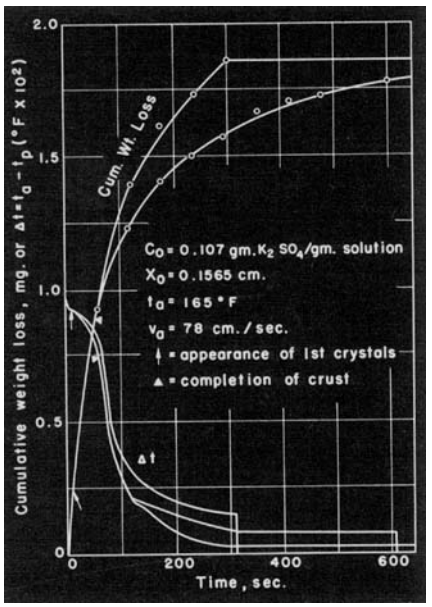

Fig. 13. Drying of several drops of potassium sulfate solution.

fractured the crust. This allowed air to enter the particle, and the liquid-vapor interface returned to the crust surface under the influence of capillary forces. Further formation of solid occurred as a crystal "fur" growing either out from the particle surface (sequence II*b*) or within the crust structure (sequence II*a*) or both. During this formation the break in the solid shell was sometimes closed, disrupting the supply of air to the particle center. If such was the case, the liquid interface once more retreated into the crust interstices, approximating the condition existing before the crust fracture occurred. If no additional breakdown of the shell occurred, the solid which formed as a result of the continued drying was deposited within the crust or on its inside surface. As the amount of liquid diminished, successively smaller pores were emptied. Once a pore pathway between the outer and inner shell surfaces was emptied of liquid, air could enter the core of the particle forming an air bubble at its center. If the crust was transparent or translucent, the bubble could be observed to grow. Solutions of ammonium sulfate, sodium sulfate, copper sulfate, and ammonium nitrate exhibited the characteristics of sequence II.

If the solid which encased the drop formed a pliable and relatively impervious skin (sequence III), the decrease in particle volume which resulted from drying after completion of the skin caused it to dimple or wrinkle. This behavior was observed in the drying of coffee extract and in the early stages of the drying of ammonium nitrate, sodium acetate, and ammonium chloride solutions. Rupture by implosion could eventually

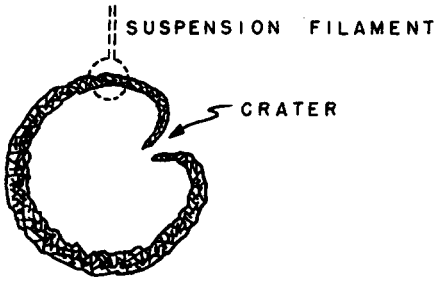

Fig. 14. Cross section of potassium sulfate particle.

occur as the skin thickened and stiffened.

Somewhat different results were observed after the closure of the crust about the droplet, if the surrounding air temperature was appreciably above the boiling point of the solution. The slowing of the mass transfer rate as a result of the additional mass-transfer resistance offered by the crust allowed the particle temperature to approach that of the surrounding air. When the boiling point of the solution was reached, vapor formed and a positive pressure was created within the particle. What effect this pressure had depended on the nature of the solid shell. If the structure was very open (sequence IV), the liquid was merely forced through the pores to the surface, where it quickly evaporated. If the crust was not sufficiently permeable to allow easy passage of the liquid, pressure built up within the particle. Under this internal stress rigid crusts (sequences V) usually fractured and plastic ones (sequence VI) inflated. In the latter case the stretching sometimes increased the skin permeability to a sufficient degree to allow the needed transmission (sequence VI*b*). If not, the skin ruptured, then collapsed (sequences VI*a* and VI*c*). Observed examples of these classifications were sodium chloride, copper sulfate (V*a*), ammonium sulfate (V*b*), lithium hypochlorite, sucrose, ammonium sulfate (VI*a*), potassium nitrate, whole fresh milk, dispersion of polyvinyl acetate (VI*b*), and coffee extract (VI*c*).

In virtually all cases the final particle consisted of a hollow, thin, nearly spherical crust. The outer surface was usually quite smooth, whereas the inner surface was rough and uneven.

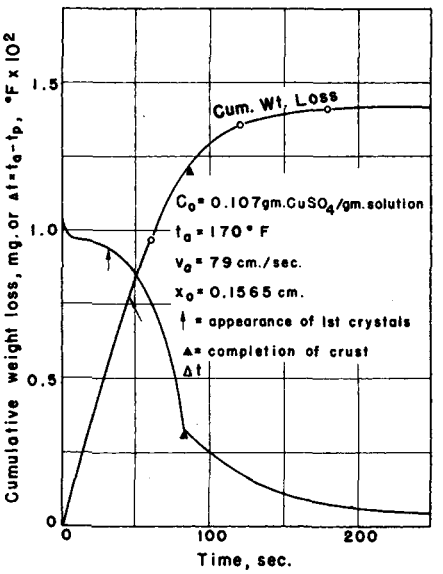

Fig. 15. Drying of droplets of copper sulfate solution.

Occasionally the inner core contained an open network of large crystals.

General Forms of the Weight-Loss and Temperature vs. Time Curves

When a droplet of pure solvent was evaporated, the cumulative weight-loss vs. time relation that was obtained was a smooth curve, concave downward and of increasing curvature. The temperature-time curve was a horizontal straight line until the droplet became extremely small, when the external effects of the suspension filament and the thermocouple became appreciable.

Early in the drying of a droplet of an aqueous solution of an inorganic salt which had little effect on the vapor pressure, the cumulative weight-loss-vs.-time curve, closely followed the curve for a pure-water droplet of the same initial volume. Generally the coincidence of the weight-loss curves for droplets of water and of

solutions persisted past the first formation of the solid phase and almost to the completion of the crust.

At the start of drying, the temperature of a droplet of solution was only slightly above that of a water droplet evaporating under the same conditions. The extent of the difference was dependent on the relative lowering of the vapor pressure by the dissolved salt. As evaporation continued and the surface layer of solution became more concentrated, the drop temperature rose slowly. The rate of rise increased somewhat with the first appearance of the solid phase and increased rapidly as the crust sometimes revealing a liquid surface or the hollow interior of the particle. These fractures were reflected in the weight and temperature curves by the sharp breaks in the second-period portion of the curves as shown in Figures 6, 8, 9, and 10. Greater initial solute concentrations increased the tendency of the crust to fracture. If the final particle were crushed and observed under the microscope, it was found to be a thin-walled hollow sphere with a crust thickness about one twentieth of the particle diameter. The outside of the shell was quite smooth, excluding any furry growth, whereas the inner surface was rough and jagged.

The weight-loss curves obtained from the drying of droplets of potassium sulfate solution in a 165°F. air stream (Figure 13) were exceptional in that the completion of the crust about the drop did not cause the evaporation rate to drop off too sharply. In fact, relatively fast rates of evaporation persisted until the particle was completely dry, as shown by the cumulative weight-loss curves running into their maximum values and Δt dropping suddenly to zero. Apparently the crust was quite open in structure and easily drew the liquid from the interior to the outer

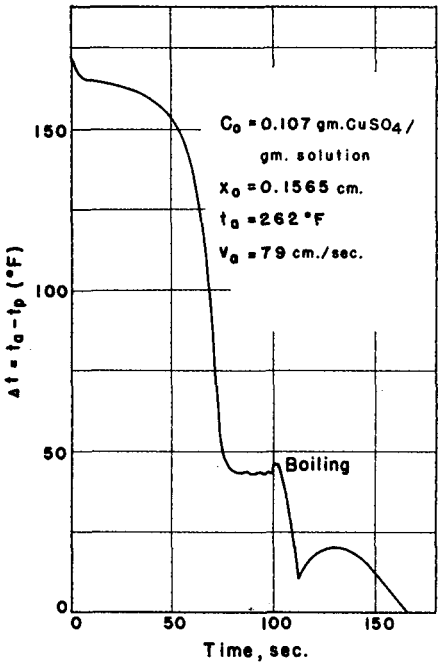

Fig. 16. Drying of droplet of copper sulfate solution in 262°F. air.

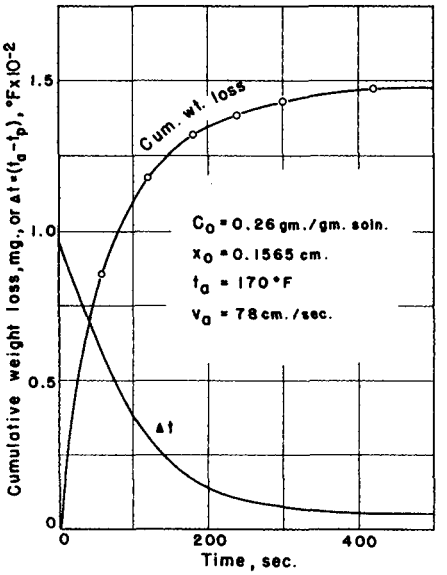

Fig. 17. Drying of droplets of coffee extract.

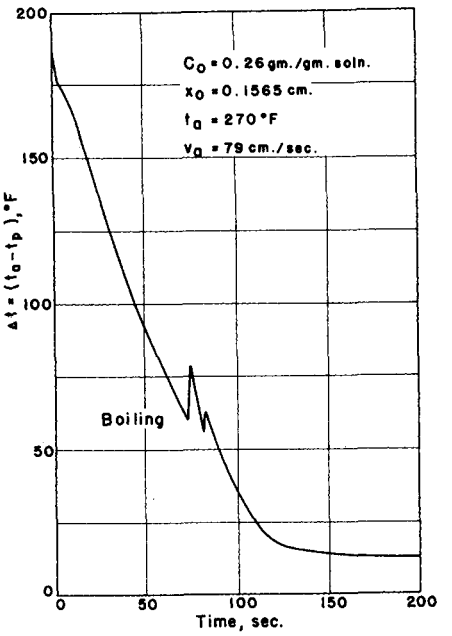

Fig. 18. Drying of droplet of coffee extract in 270°F. air.

neared completion.

Curves of Weight Loss and Temperature vs. Time

Figures 5 to 13 and 15 to 19 are specific examples of the weight-loss and temperature curves obtained in this study. Additional examples are given in the thesis (*1*) on which this paper is based. The weight-loss curves were experimentally measured weight-time relations, while the Δt curves were derived from the continuous chart records, smoothed to remove the effect of the rapid oscillations of air temperature. A reproduction of an actual temperature is given in Figure 20.

The data obtained for the drying of drops of sodium sulfate solutions under various conditions are shown in Figures 5 to 10. In a majority of the droplets dried there was some inward collapse of the solid shell after it had formed,

Figure 11 shows the data for the drying of ammonium nitrate solutions of three different initial concentrations expressed as cumulative weight loss against the elapsed drying time. Not only was more water removed in a given time from the droplet of lower initial concentration, but also the particle so formed approached dryness more quickly. It was also noted that at the moment the crust was completed the average concentration of the particle was approximately the same no matter what the initial concentration or the drying conditions.

The temperature behavior of droplets of ammonium nitrate solution evaporating under various conditions is shown in Figure 12. Immediately after the first crystals had formed, the Δt between air stream and particle dropped off quite rapidly. At least part of this effect can be ascribed to the large heat of crystallization of ammonium nitrate.

surface. So rapid was this flow that the crust did not have time to completely cover the droplet. As the crust neared completion, the liquid was drawn away from the open area, leaving a sizable crater in the crust. When fractured and viewed under the microscope, the dried particle proved to be a very thin shell composed of large crystals. A cross section of the shell through the crater is shown in Figure 14.

The crust formed upon the drying of droplets of copper sulfate solution was of low permeability, as is evidenced by the flattening of the cumulative weight-loss curve (Figure 15) soon after the completion of the solid shell. During the drying of one particle the crust fractured, and immediately the drying rate jumped to an appreciably higher value and maintained it until the particle reached a composition equivalent

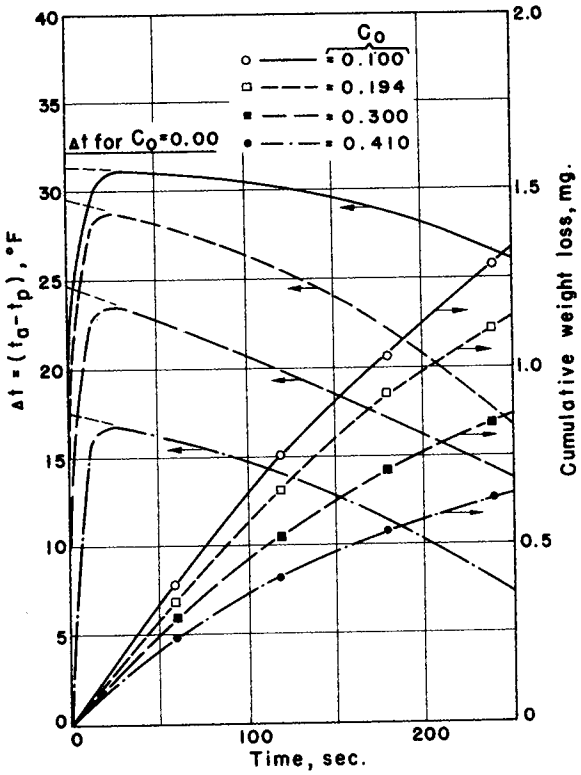

Fig. 19. Effect of concentration on drying aqueous calcium chloride drops x_o = 0.1565 cm., t_a = 81°F., v_a = 95 cm./sec.

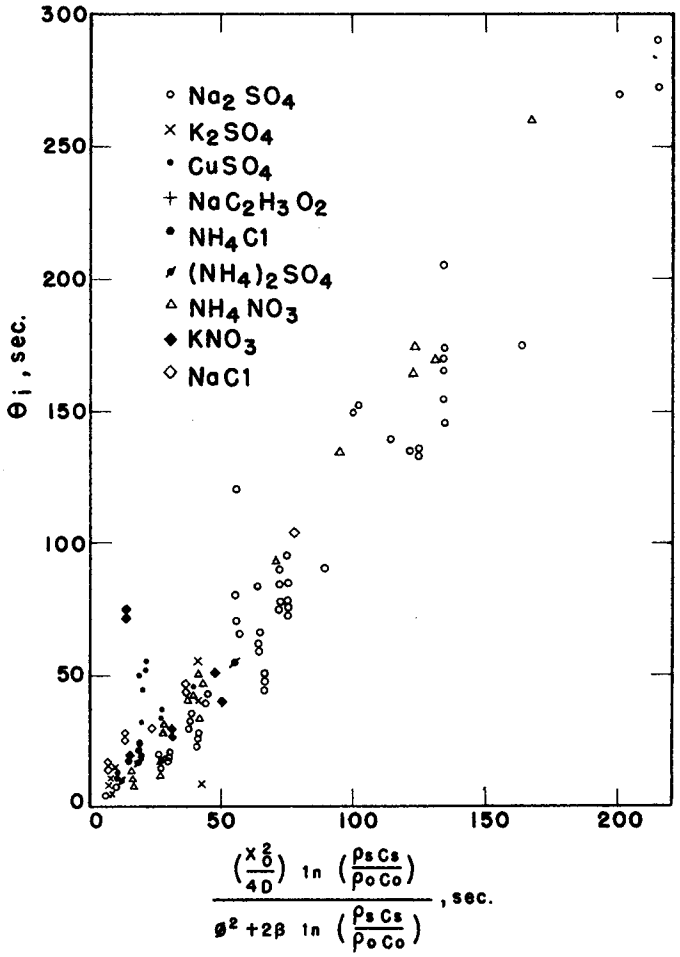

Fig. 21. Correlation of first appearance of crystals by Equation (12).

to the pentahydrate. This indicated that before the fracture of the crust the evaporation rate was controlled by the diffusion of vapor from the liquid-vapor interface through the crust to the particle surface. In a 262°F. air stream a solid crust quickly formed about the drop. The particle temperature reached the boiling point, and the particle bubbled vigorously, fracturing the crust at several points. The final particle was white, shiny, and quite smooth. The Δt time curve is shown in Figure 16.

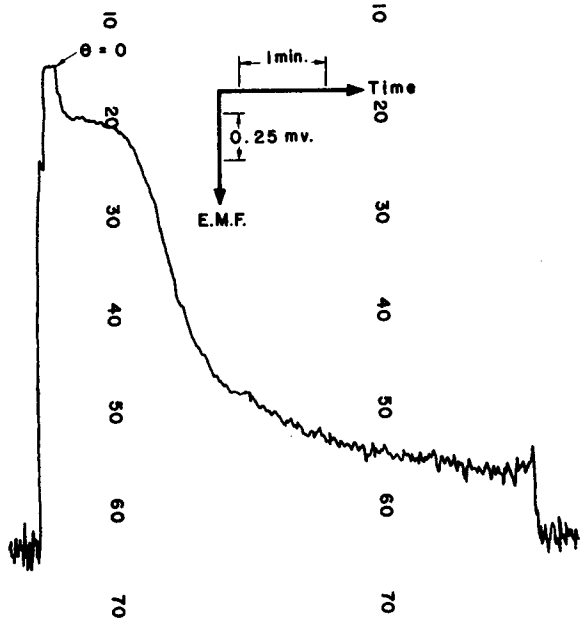

Fig. 20. Sample temperature-vs.-time data from recorder-strip chart.

When dried below the boiling point, a droplet of coffee extract first skinned over and then shriveled. The skin acted as a pliable sack suspended from the filament. As more and more of the liquid was evaporated, the upper portions of the skin wrinkled and the particle became longer than it was wide. Weight-loss and Δt curves are given in Figure 17.

If the air temperature was above the boiling point of the extract, the final dried particle took on a completely different appearance. It first shriveled in a manner similar to that described above. When the droplet reached the boiling point, internal vaporization inflated the surface skin until rupture occurred. The skin then repeatedly inflated and collapsed, forming a spongy structure. Each small bubble in the

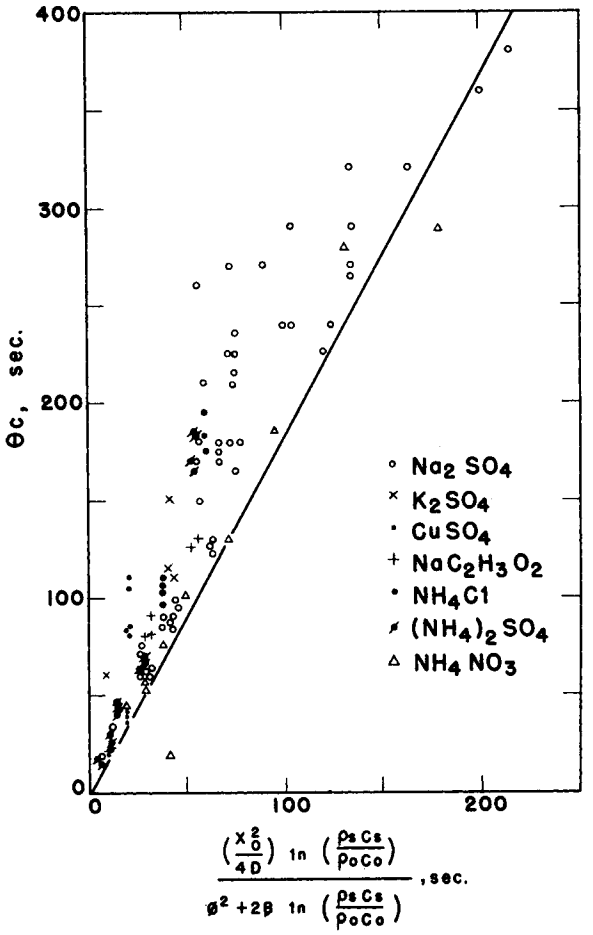

Fig. 22. Correlation of time of crust completion by Equation (12).

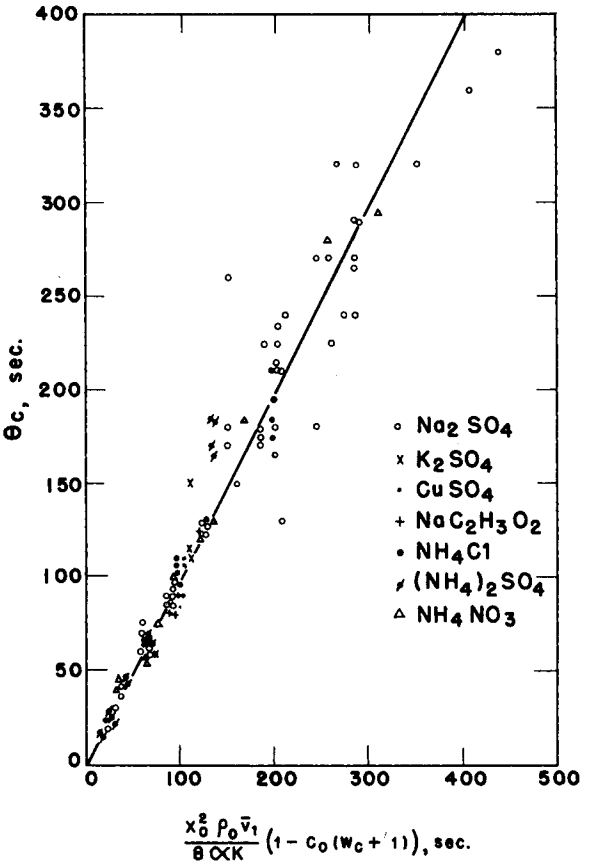

Fig. 23. Correlation of time of crust completion by Equation (14).

final dried particle appeared to be the result of one cycle of inflation and collapse. The temperature history of a droplet dried in air at 270°F. is given in Figure 18.

Surface Concentrations

Ranz and Marshall (*10*) suggested that droplets of solutions evaporated at all times as if they were saturated, even though the average solute concentration in the droplet was well below the saturation value. To test this hypothesis, a number of measurements of droplet weight loss and temperature were made with calcium chloride solutions of four different initial concentrations. The results are plotted in Figure 19. Pronounced differences in droplet temperatures and evaporation rates were noted between the droplets of different initial concentration. It is thus apparent that droplets of all aqueous solutions of any concentration do not necessarily evaporate as if saturated.

Formation of a Solid Phase in Drying a Droplet of Solution

The time of the formation of a solid phase around a drying droplet is important since it limits the period of relatively rapid drying. It also has an important bearing on the size and properties of the final dry product.

In all but a few of the runs in which droplets of salt solutions were dried, the times of appearance of the first crystals and of the completion of a

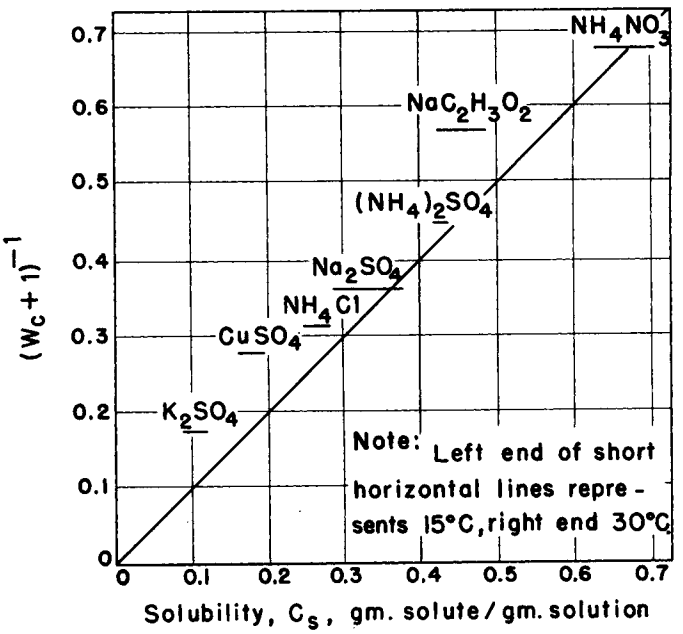

Fig. 24. Variation of the parameter W_c with solute solubility.

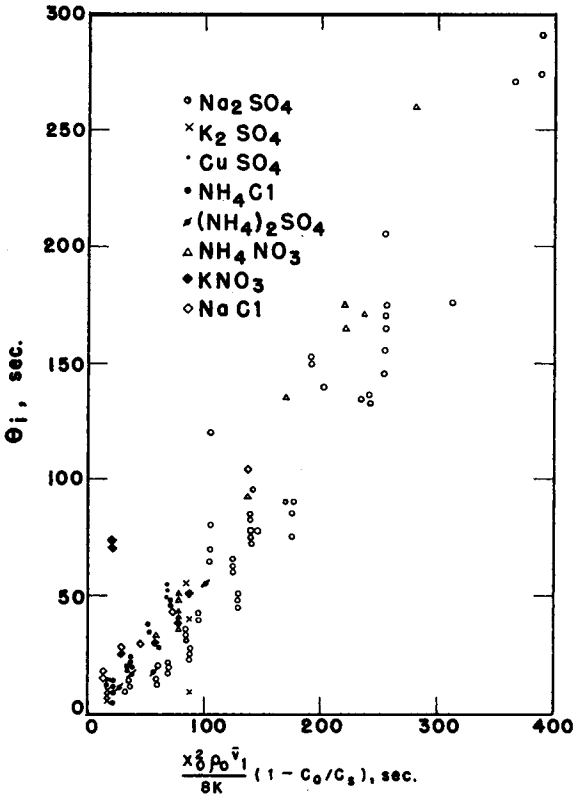

Fig. 25. Correlation of first appearance of crystals by Equation (16).

solid crust about the droplet were noted. These results were correlated by means of Equation (12). Figures 21 and 22 show the observed time of formation of the first crystals and of the completed crust, respectively, plotted against the value calculated from Equation (12). In Figure 22 a straight line having the equation

$$\theta_c = \frac{1.84x_o^2 \ln\left(\frac{\rho_s C_s}{\rho_o C_o}\right)}{4D\left[\phi^2 + 2\beta \ln\left(\frac{\rho_s C_s}{\rho_o C_o}\right)\right]} \quad (13)$$

has been drawn along the minimum bound of the data.

In the calculation of values of θ_c from Equation (12) the following practical assumptions were made: (1) the droplet was at the wet bulb temperature, (2) the initial evaporation rate was equal to the rate of evaporation of a pure-water droplet of the same size as calculated from the mass transfer correlation of Ranz and Marshall (*10*), (3) K was evaluated at initial conditions, and, (4) the partial specific volume of water in the solution was assumed to be 1.0 cc./g.

A severe limitation on the accuracy of the calculations is imposed by the lack of reliable data for the diffusivities of salts in aqueous solution. Most data in the literature are reported as average values for concentration ranges from fixed values of infinite dilution. The values used in the calculations were based on those reported in the International Critical Tables adjusted as well as possible to the experimental conditions of concentration and temperature.

From the results of the runs in which the weight loss from the drops was measured, it was noted that for any one solute the average moisture content of the particle at the time of crust completion had approximately the same value for all droplets dried and was apparently independent of initial droplet diameter, initial solute concentration, and drying conditions. If this is assumed always to be true, the following expression for θ_c can be derived:

Table 1. Values of the Parameter W_c for Various Solutes

Solute	W_c, lb./lb. dry solid
Sodium sulfate	1.75
Potassium sulfate	4.32
Ammonium nitrate	0.45
Copper sulfate	2.47
Sodium acetate	0.70
Ammonium sulfate	1.22
Ammonium chloride	2.20

$$\theta_c = \frac{x_o^2 \rho_o \bar{v}}{12\alpha K}[1 - C_o(W_c + 1)] \quad (14)$$

For the solutes studied, an average value of α was found to be 0.67. Table 1 lists values of W_c chosen so that values of θ_c calculated from Equation (14) would best fit the experimental data.

In Figure 23 the observed values of θ_c are plotted against those calculated from Equation (14) with the parameters of Table 1. Agreement is quite good between observed and calculated values. However the correlation seems more coincidental than logical. It is quite evident that it will not yield satisfactory results at conditions greatly removed from those under which the experiments were carried out; for instance, it would be expected that, if the initial solute concentration were equivalent to the saturation value at the evaporating temperature, the solid crust would form immediately. To predict this the term $[1 - C_o(W_c + 1)]$ in Equation (14) must equal zero if C_o is the saturation value. Consequently, since solubility varies with temperature, W_c must also if the correlation is to hold for all temperatures. Such a dependency could not be detected in the experimental results. From solute to solute, however, W_c does seem to be related to solubility as is indicated in Figure 24. If the relation represented by the 45-deg. line in Figure 24 is used for the approximation of W_c values, Equation (14) may be used without the need of experimentally determining parameter values. Also, a zero value of θ_c is then indicated for droplets initially saturated. The equation of the 45-deg. line of Figure 25 is

$$(W_c + 1) = \frac{1}{C_s} \quad (15)$$

Inserting Equation (15) into Equation (14) gives

$$\theta_c = \frac{x_o^2 \rho_o \bar{v}}{8K}[1 - (C_o/C_s)] \quad (16)$$

Figures 25 and 26 show the observed time of the formation of the first crystals and of the completed crust, respectively, plotted against values calculated from Equation (16).

Final Particle Diameters

The final dried particle was not always spherical, and consequently its final volume was difficult to estimate. Within the experimental error the decrease in the volume of particles from initial droplet to dried particle, when drying was carried out at temperatures below the boiling point, was equal to the volume of the water evaporated before the completion of the solid crust. For drying at temperatures above the boiling point insufficient data were

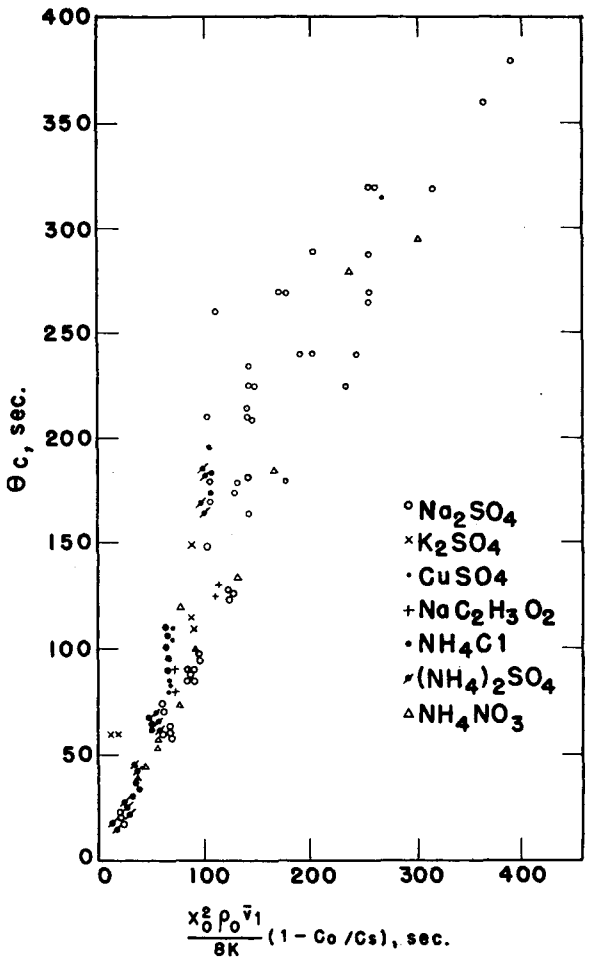

Fig. 26. Correlation of time of crust completion by Equation (16).

obtained to justify any conclusions. In many cases the final particle was larger than the original droplet because of inflation of the crust by internal pressure. The amount of inflation varied from particle to particle, even though drying conditions were constant. Some materials, such as sodium sulfate, showed little expansion under any circumstance.

Circulation Within Drying Droplets

Evidence of liquid movement was noted during the drying of a number of the droplets. However since with few exceptions the circulation appeared to be either on the surface or parallel to it, the movement may be attributed to either circulation within the droplet or rotation of the droplet as a whole. The majority of the observations seemed to indicate the latter. The particles of solid phase which formed during the drying frequently moved about on the droplet surface but were never observed to move into the interior. This does not negate a radial movement of the liquid but may only be an indication of the effect of surface tension and concentration gradients. However on the few occasions when dust particles were observed within the droplet, their motion always appeared to be parallel to the surface.

NOTATION

B = constant in falling-rate equation $= R'_o/W_c$
C = solute weight fraction, g. solute/g. solution
c = concentration, g. solute/cc. solution
D = diffusivity, sq. cm./sec.
F = fraction of initial water removed
H = humidity, lb. water/lb. dry air
h = heat transfer coefficient, cal./(sec.) (sq. cm.) (°C.)
K = evaporation constant, sq. cm./sec.
k = thermal conductivity, cal./(sec.) (sq. cm.) (°C./cm.)
L = vertical distance along spray-dryer axis
m = weight of droplet, g.
N_{Nu} = Nusselt number for heat transfer $= hx/k$
R'_o = rate of evaporation in constant-rate period
r = distance from center of drop
s = weight of total solute in droplet, g.
t = temperature, °C.
v = velocity, cm./sec.
$\bar{v}$ = partial specific volume, cc./g.
W = moisture content, lb. water/lb. dry solid
w = weight of water in droplet, g.
W_c = constant for any particular solute, moisture content
x = diameter of droplet, cm.

Greek Letters

α = constant for any particular solute
$\alpha_n (n=1,2,3\ldots)$ = positive real roots of tan $z = z/(\beta+1)$
β = dimensionless ratio $= K/D$
θ = time variable, sec.
θ_c = time for completion of solid crust
λ = latent heat of vaporization, cal./g.
ρ = density, g./cc.
ϕ = positive real root of tanh $y = y/(\beta+1)$

Subscripts

a = air stream
c = value at instant of crust completion
d = value for dried particle
i = value at instant of appearance of first crystal
m = mean value
o = initial condition
s = value at saturation
t = value at terminal velocity

PART II

The practical value of the observations and correlations reported in Part I of this paper is their applicability to design calculations. In the following numerical example illustrating their use it has been necessary, since much information is not yet available concerning many phases of the spray-drying process, to make reasonable estimates and simplifying assumptions in order to give continuity to the calculations.

A spray dryer operates under the following conditions:

Inlet	Air temperature,	500°F.
	Humidity,	0.010 lb. water/lb. dry air
Outlet	Wet-bulb temperature,	126.5°F.
	Air temperature,	280°F.
	Humidity,	0.060 lb. water/lb. dry air
	Wet-bulb temperature:	126.5°F.

(Negligible heat losses assumed)

Feed	Solute, sodium sulfate Initial solute concentration, 20.0% by weight
Drop size	Distribution, log-probability, by volume Volume median drop size, 100μ Minimum drop size (at 1% level), 40μ Maximum drop size (at 1% level), 250μ

If Equation (15, Part I) is assumed to hold, the moisture content of a particle at time of crust completion equals 2.16 lb. of water/lb. of sodium sulfate. Then the fraction of water removed by the time of crust completion equals

$$\frac{4.0 - 2.16}{4.0} = 0.46$$

If the spray has a homogeneous drop size, then the humidity at crust completion time is $H_c = 0.010 + 0.46(0.060 - 0.010) = 0.033$ lb. of water/lb. of dry air. This corresponds to an air temperature, t_{ac}, of 390°F. For calculation of the time of crust completion, the air conditions may be taken as an average of the initial values and those at crust completion. Hence

$$t_{am} = \frac{500 + 390}{2} = 445°\text{F.}$$

Wet-bulb temperature = 126.5°F.
Humidity (corresponding to above temperatures)
= 0.0223 lb. of water/lb. of dry air

The drops are assumed to have a velocity relative to the air equal to their terminal velocity; then K may be evaluated.

From Equation (13) the crust completion time may be calculated for particular drop sizes; hence

x_o, μ	40	100	250
θ_c, sec.	0.027	0.14	0.53

On the basis of these figures, the spray tower should be designed so that the airflow pattern keeps the spray droplets away from the walls for at least 0.6 sec. after atomization to prevent solid buildup on the walls. Likewise, if there are eddies present around the nozzle which will entrain the fines, there is likely to be buildup if airborne time is less than 0.03 sec.

If it is assumed that the final particle size is the same as the droplet size at the time of crust completion, as appears to be the case with salts as sodium sulfate, then the final particle density and diameter may be calculated.

The amount of evaporation taking place before crust completion can be calculated from the correlations for the drying rate and the completion of the solid crust. The fraction of the initial water removed by crust completion time can be calculated as

$$F_c = \frac{-\left(\frac{dm}{d\theta}\right)_m \cdot \theta_c}{\text{initial water in droplet}} = \frac{0.67\left(\frac{dm}{d\theta}\right)_o \cdot \theta_c}{\frac{\pi}{6} x_o^3 \rho_o (1 - C_o)}$$

$$= \frac{\pi k}{\lambda} \cdot x_c N_{Nu} \cdot \left(\frac{t_a - 212}{1.8}\right)$$

The Nusselt number is evaluated at the terminal velocity of the particle at the instant of crust completion.

Expressed in terms of moisture content, $-(s/B)(dW/W) = d\theta$, where $s = (\pi/6)\rho_o x_o^3 C_o$; hence $\theta = \theta_o + (s/B)\ln(W_o/W)$. This equation gives a relationship between moisture content and drying time. From this can be obtained a relationship between moisture content and distance fallen, if plug flow of air in the tower is assumed.

For any particular particle size

$$L = \int_0^\theta (v_t + v_a)\, d\theta$$

The terminal velocity v_t may be evaluated at an average temperature, since the mean film temperature varies to a much lesser degree than either the particle or air temperatures. For this example v_a, the net downward air velocity in the tower, is taken as 1.5 ft./sec.

The equations may then be applied to the heterogeneous spray, with the approximate temperature profile assumed. This yields a more exact profile. The procedure may then be repeated if necessary.

To apply this method to the numerical example, the original spray was divided into five size classes, equal in volume, the behavior of each class being taken as that of its own median-diameter droplet. The moisture contents as functions of time and of position were determined for the five size classes and for the minimum and maximum droplet sizes. These are plotted in Figures 27 and 28, the resulting temperature profile is plotted in Figure 29.

To carry out this procedure for a heterogeneous spray, it is first necessary to determine an approximate temperature profile in the tower, preferably by carrying out the procedure on the assumption of a homogeneous spray of droplets with diameter equal to the median droplet diameter in the real distribution, that is 100μ for the numerical example treated here.

Assuming that there is no mixing in the tower and that plug flow of air exists one can obtain from the temperature profile an indication of the highest temperatures to which the solid is exposed. This is based on the observation that soon after the solid phase covers the droplet the particle temperature rises sharply toward the air temperature. From Figure 29 it can be seen that the fines might reach 477°F. and that the majority of the particles will be exposed to 350°F.

In these calculations the values used for the crust completion times were the minimum values to be expected. Experiment has shown that the first drying period may persist considerably longer than these values would indicate, but use of the minimum values is preferable, as they represent the worst picture of the process from the drying point of view. A longer duration of the first drying period for a portion of the particles than that assumed would result, in practice, in a lower temperature exposure and a

The final particle diameter and particle density are then

$$x_d = x_o \left\{ \frac{\rho_o}{\rho_c} [1 - F_c (1 - C_o)] \right\}^{1/3}$$

$$\rho_d = \frac{C_o \rho_c}{1 - F_c (1 - C_o)}$$

For this example numerical results are

x_o, μ	ρ_d, g./cc.	x_d, μ
50	0.350	43.5
100	0.346	87.5
250	0.327	223

Although information on solid-phase formation and product properties is very important for design considerations, a major need is a method of predicting drying times and tower height required for a product of the desired moisture content.

Two drying periods, somewhat analogous to those in tray drying, must be considered in the drying of a spray droplet. The first period is characterized by evaporation from a free liquid surface, and the second by evaporation from or through a solid structure.

The amount of drying taking place in the first period has already been discussed. No extensive data were taken on evaporation rates during the second period. However a linear relationship between evaporation rate and moisture content is common in tray drying, and it is reasonable to assume that such a relationship may be employed to give a first approximation as to rates during the second period of spray drying, provided the proper proportionality constant is used and the particle size does not change appreciably once the solid crust is completed.

As the second period of drying begins in high-temperature drying, the particle temperature is usually near the boiling point of the solution. On the basis of this fact, the calculated particle size, and the heat transfer correlation for spheres (*10*), it is possible to calculate the drying rate at the start of the second period. This enables the estimation of the proper proportionality constant between the drying rate and the moisture content.

For the second period

$$-\frac{dm}{d\theta} = BW$$

where

$$B \frac{R'_o}{W_c}$$

and

$$W_c = (1 - F)\, W_o$$

$$R'_o = \frac{hA\Delta t}{\lambda} = \frac{kN_{Nu}}{x_c} \pi x_c^2 \frac{\Delta t}{\lambda}$$

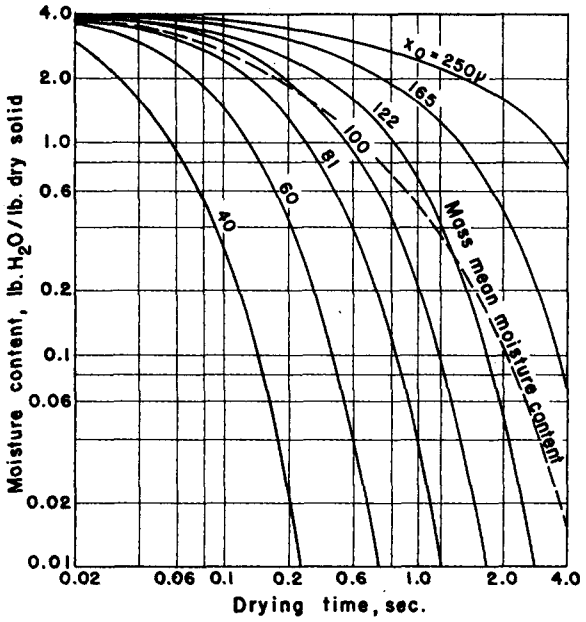

Fig. 27. Variation of moisture content for droplet of sodium sulfate solution with time in a spray dryer.

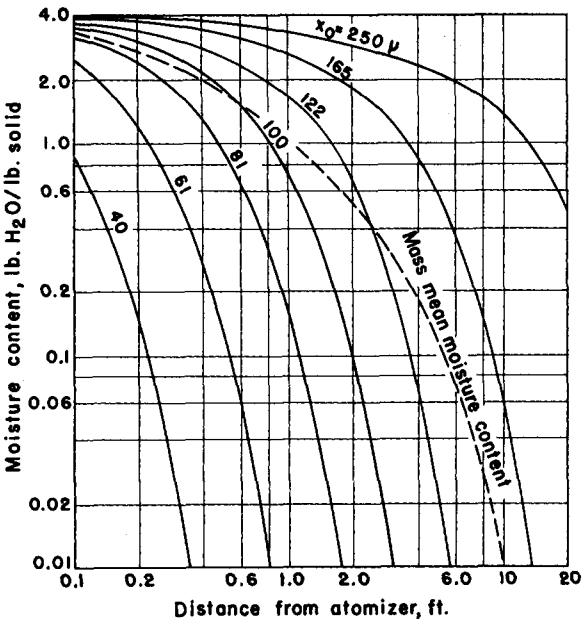

Fig. 28. Particle moisture-content profiles in a spray dryer.

drier product. The only design factor in which a maximum length of the first period might be considered is the air-borne time necessary to prevent buildup on the dryer walls. In the numerical example considered here it would be preferable if dryer size and air-flow pattern were adjusted so that no particle reached the walls in less than 1 sec.

DISCUSSION OF RESULTS

The First Period of Drying

The first period of drying is characterized by evaporation from a free liquid surface. It is natural therefore to compare the evaporation during this period with that taking place from a pure-water droplet. It is doubtful that, as discussed earlier, the assumption of Ranz and Marshall (*10*) that a drop of solution evaporates at all times as if it were saturated, regardless of the average solute concentration in the droplet, is realized in practice. The results of the drying of droplets of calcium chloride solutions seem to confirm this (Figure 19). Apparently the surface concentration rises from its initial value toward the saturation value in a manner similar to that predicted by Equation (8). Consequently the evaporation rate during the first period of drying is less affected by the change in vapor pressure caused by the presence of the solute than would be predicted by the use of the Ranz and Marshall assumption. Also since the majority of salts have only a small effect on vapor pressure, even when present at saturation concentrations, from the standpoint of practical usage rather than theory the increased difficulties to calculation introduced by taking into account a vapor pressure changing with time would not be justified. Except in the drying of solutions of materials, such as calcium chloride, which have a very marked effect on the vapor pressure, it is preferable to assume that the evaporation rate for a solution is the same as that for a pure-water droplet. Greater errors are usually introduced in assumptions concerning the relative velocity of the droplet with respect to the air, especially immediately after atomization, and the air temperature and humidity.

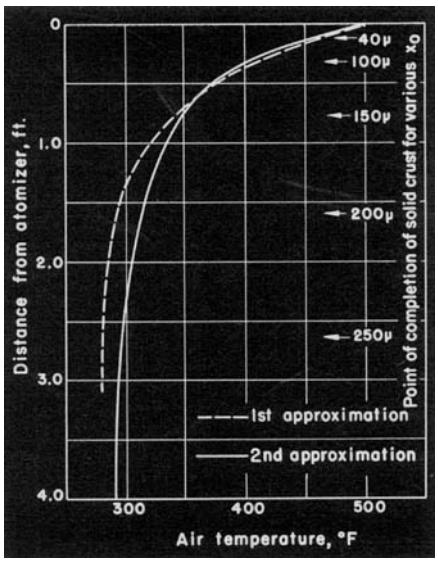

Fig. 29 Calculated temperature profiles in a spray dryer.

A similar argument can be advanced for the use of the wet-bulb temperature as that of the evaporating droplet.

Examination of Figures 9 and 11 shows the approach to equivalence of evaporation rates from droplets of solutions and water initially of the same size. It will be noted that the rate from a droplet of solution remains close to that from a water droplet even after the solid phase has appeared and almost until the droplet is covered with solid. The solid crust is evidently sufficiently porous so that its surface remains wetted and continues to expose a liquid surface to the air stream. From the combination of weight-loss and temperature data it can be shown that during this period the heat transfer coefficient does not show any changes not attributable to the changes in the droplet diameter and temperature. This is further evidence that the liquid interface remains close to the particle surface until the crust completely covers the droplet.

The Formation of the Solid Phase

The solid-phase formation data as plotted in Figures 22, 23, and 26 show considerable scatter. It is reduced to some extent in Figure 23, since the correlating Equation (14) contains an empirically adjusted parameter. No form of correlating equation, however, could remove all the scatter, since the observed times for crust completion for consecutive runs under identical conditions varied as much as ± 15% from the mean. The usual variation was about ± 7%. A good deal of the scatter of the data can be attributed to natural randomness inherent in the crystalliza-

tion of the crust, the circulation in the drop, and the movement of the partially formed crust about the surface of the drop. Consequently it obscures in small samples the average behavior of a droplet. The fact that such a spread does occur must be considered in analyzing the behavior of a spray. Even though for computing temperature profiles, for example, the large number of droplets could be considered as having an average behavior, the extreme variations from the mean would have to be considered if it were essential that all particles reach a certain level or dryness.

A droplet suspended and drying under the conditions used in this investigation is stabilized to a large extent by the density gradients which accompany the concentration gradients. The solid phase is formed first at the bottom of the droplet and moves progressively up its sides until the entire surface is covered. In a commercial dryer, however, spherical symmetry is approached in the droplets because of rotation induced by atomization and turbulent air. In addition, for free-falling droplets less than 100μ in diameter the terminal velocity is too small to have a significant effect on evaporation rates (*10*). Since the experimental data were taken in a situation in which spherical symmetry was definitely not present and must be applied to one in which it is, direct equivalence cannot be assumed. However it is possible to estimate qualitively the effects of the different conditions and to arrive at a conclusion which is probably as accurate as other uncertainties warrant.

The evaporation rates around a droplet with an air stream impinging on it from one direction are not uniform but vary from a maximum at the point of impingement through a minimum to a second, but smaller, maximum at the opposite pole. A solid phase is formed first in the region of highest evaporation rate and appears sooner than if the mean rate prevailed over the entire surface. Similarly in the areas in which the evaporation rate is lower than the mean, the solid will form later than it would under uniform conditions. Experimentally two periods of time were recorded for each drying droplet, that at which the first solid appeared and that at which the crust completely covered the drop. Theoretically for a droplet having perfect spherical symmetry these two times would coincide. That value would lie between the two experimental values, other factors being equal; the other factors would include circulation within the drop and supersaturation of the surface, as well as the more obvious and easily measured ones of temperature, drop size, initial concentration, etc. It seems more than coincidental that the experimental values of θ_o, as plotted in Figure 22, exhibit a minimum bound equal to 1.84 times the value of θ_c calculated from Equation (12). This bound lies between the values of the times for the appearance of the first crystals and those for the completion of the crust. It is suggested, therefore, that its use would give a good estimate of the time of completion of a solid crust about a free-falling droplet. In the light of some results of Ranz and Marshall this choice seems sound. They dried a droplet of ammonium nitrate solution suspended in still air. Since there was no imposed air velocity, the evaporation rates about the droplet should have been almost uniform. They observed a crust completion time of 600 sec.; the value calculated from Equation (13) is 606 sec.

The final decision as to the soundness of the choice of Equation (13) and of its accuracy must be left until a technique is developed whereby observations, similar to those made in this investigation, can be made for free-falling droplets.

The Second Period of Drying

Drying rates in the second period showed so much variation from particle to particle, even though they were dried consecutively under identical conditions, that a quantitative analysis of the results is impossible. For example, the results of the drying of three droplets of potassium sulfate solution, given in Figure 13, indicate a severalfold variation in total drying time. However the data serve to point out some of the factors involved in the drying process in the second period and give an insight into the physical phenomena which occur.

In the spray drying of a solution, unlike the tray drying of granular and slab materials, the properties of the structure through which the moisture must move are not predetermined. They are dependent not only on the nature of the material being dried but also on the conditions under which the solid is deposited from solution. The previous history of a particle plays a large role in determining its subsequent drying. A factor such as the air velocity past the particle, which ordinarily would be expected to have only a minor effect on drying occurring within a porous structure, may have a large indirect effect as a factor determining the dimensions and nature of that structure.

Some information with regard to moisture movement in the drying particle can be deduced from the experimental observations. The data for the drying of droplets at temperatures less than the boiling point show that the heat transfer coefficient drops markedly at the end of the first period of drying. This indicates an added resistance to transfer of heat from the air stream to the liquid-vapor interface, a result of the retreat of the interface into the interstices of the solid crust. Visual evidence of this retreat was a twinkling, frequently seen in the crust as the liquid withdrew. The retreat of the interface results from the inability of the particle to supply liquid to the surface at a rate equal to the evaporation rate from a continuous liquid surface. The crust is rigid and cannot contract as liquid is removed from the particle. Therefore the liquid will move to the surface from the core of the particle only if the core is supplied with air from without or internal vaporization occurs under an internal pressure reduced by the capillary forces. At sub-boiling-point temperatures the latter is difficult to realize. If a continuous pathway through the crust, empty of liquid, is not available to permit the passage of air into the particle core, then the volume decrease resulting from evaporation must be compensated for by a retreat of the vapor-liquid interface into the crust. If the withdrawal is sufficient, the necessary pathway may be opened for air to enter the core. This will allow the capillary forces once more to draw the liquid to the particle surface, the result of which will be a rise in evaporation rate to a value comparable to that existing at the end of the first drying period. A fracture of the crust by surface tension or other forces will have the same result as the emptying of a pathway. Once a pore is emptied or the crust fractures, admitting air to the particle core, the moisture is susceptible to movement through the crust under the influence of capillary forces. The situation is complicated by the continual deposition of solid in the crust structure. It is thus possible that the entrance for the air can be sealed off and the cycle repeated.

Further experimental evidence of the occurrence of the events postulated above appears in Figure 10. Similar observations of the return of drying rates to high values were reported by Ernst *et al.* (3) in connection with tray-drying studies. They found that shortly after the falling-rate period of drying had begun, the breaking of the seal at the bottom of the trays by the admittance of air caused drying rates to rise sharply.

Since the moment when a pore will open or the crust will fracture to admit air to the particle depends, in part, on the structure of the crust, which itself is quite random, drying rates in the second period are very unpredictable.

As a result few general conclusions can be drawn. In addition the weakening effect on the crust because of the presence of the suspension filament cannot be discounted.

The situation is little improved at air temperatures above the boiling point. If the particle reaches the boiling point, internal vaporization occurs, and it is no longer necessary for air to be admitted to the core. However the internal pressure frequently fractures the crust, and the further history of the drying becomes dependent on the nature of the fracture. In addition experimental measurement becomes more difficult and, as a result, less accurate. Each of the factors of crust structure, crust strength, and rigidity, crystal form, etc., which are unique properties of the material dried, become of major importance in determining the drying rate and final particle characteristics. Further work is necessary to establish their effect on the drying process.

A few indications of the results to be expected may be found from the data of this investigation. In Figure 11 the weight-loss curves for droplets of three concentrations of ammonium nitrate solutions show that not only was more water removed in a given time from the droplet of lowest initial concentration but also the particle so formed approached dryness more quickly. It has been noted that at the moment the crust is completed the average concentration in the particle is approximately the same no matter what the initial concentration or the drying conditions. This means that if two droplets of the same size are dried, one having twice the original solute concentration of the other, then the more concentrated one will have a particle volume at shell completion approximately twice that of the less concentrated one. The ratio of the surface areas will be about 1.6. Since the more concentrated one contains twice the amount of solid, its shell will be thicker for the same degree of dryness and will offer more resistance to transfer of water through it. When one assumes that the porosity of the crust is equal in both cases and that the evaporation rate per unit area will vary inversely as the thickness of the crust, the gross rate of evaporation from the particle which was originally more concentrated will be 1.26 times that from the originally less concentrated one. However for the same average moisture content the former will contain twice as much water. It would thus be expected that the time required, after the crust completion, to reach a certain average moisture content in the particle would be 2/1.26, or 1.51, times as long if the initial concentration were doubled. Experimentally this has been

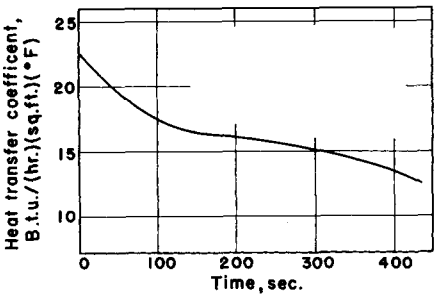

Fig. 30. Variation of heat transfer coefficient during the drying of a droplet of coffee extract.

shown to be of the right order of magnitude. It is not to be presumed, however, that the actual situation is that simple. For example, the original concentration and drying conditions probably have a significant effect on the shell porosity. It should be noted also that the total drying time, which is the final measure of the speed of the drying, depends as well on the time necessary for crust completion.

The Drying of Materials Other Than Inorganic Salts

The correlation methods which have been derived for crust formation are not applicable to suspensions and complex mixtures for which the properties of solubility and diffusivity do not exist in their normal sense. In fact, with materials such as coffee extract, it is difficult to define the transition from a liquid to a solid surface about the drop. However the process of the drying of a droplet containing inorganic salts from its initial formation to the final dried particle cannot be correlated as a whole, since the two drying periods involve different mechanisms. The periods must be treated separately as two interrelated but distinct parts of the same process. There is evidence that the drying of other materials should be treated period by period also.

Ranz and Marshall (*10*) dried droplets of whole milk and of a suspension

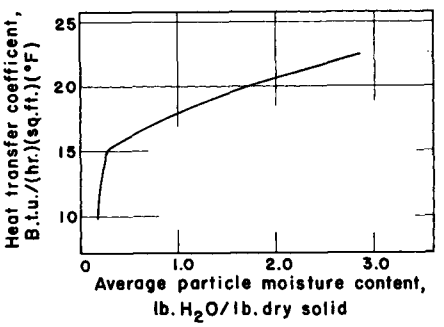

Fig. 31. Change of heat transfer coefficient with the moisture content during the drying of a droplet of coffe extract.

of dye in still air and found that they exhibited a first period during which evaporation occurred at rates which were close to the rate from a water droplet. A second period followed in which lower rates were observed.

When coffee extract was dried in this investigation, the first period of drying seemed to be absent. There was no period during which the particle temperature remained approximately constant; rather it rose steadily from the outset. Both the temperature and weight-loss curves (Figure 17) for drying at temperatures below the boiling point were smooth with no break points and would indicate that all the drying could be considered as having taken place in one period. If, however, the data are analyzed further, evidence of a change in mechanism develops.

The over-all heat transfer coefficient can be estimated from the weight-loss and temperature curves if it is assumed that the area of the particle changes as a result of the weight loss in the same manner as would a sphere. Figures 30 and 31 present the calculated values of h plotted against drying time and average particle moisture content, respectively. From Figure 31 it can be concluded that at a moisture content of 0.4 either there was a sharp retreat of the liquid-vapor interface into the particle or the remainder of the water in the particle was bound and had a higher heat of vaporization. Either explanation is plausible.

ACKNOWLEDGMENT

The authors wish to acknowledge the financial assistance of the Wisconsin Alumni Research Foundation and the Proctor and Gamble Company.

LITERATURE CITED

1. Charlesworth, D. H., doctoral thesis, Univ. of Wis., Madison (1954).
2. Duffie, J. A., and W. R. Marshall, Jr., *Chem. Eng. Progr.*, **49**, 417 and 480 (1953).
3. Ernst, R. C., *et al.*, *Ind. Eng. Chem.*, **30**, 1119 (1938).
4. Fogler, B. B., and R. B. Kleinschmidt, *ibid.*, 1372 (1938).
5. Frössling, N., *Gerlands Beitr. zur Geophysik*, **52**, 170 (1938).
6. Fuchs, V. M., *Phys. Z. Sowjet.*, **6**, 224 (1934).
7. Kirschbaum, E., *Chem. Eng. Tech.*, **24**, 3 (1952).
8. Langstroth, G. O., C. H. H. Diehl, and E. J. Winhold, *Can J. Research*, **28A**, 580 (1950).
9. Luchak, G., and G. O. Langstroth, *ibid.*, **28A**, 574 (1950).
10. Ranz, W. E., and W. R. Marshall, Jr., *Chem. Eng. Progr.*, **48**, 141 and 173 (1952)

Manuscript received August 13, 1957; revision received July 20, 1959; paper accepted August 4, 1959. Paper presented at A.I.Ch.E. Baltimore meeting.